universe

IMPACT FACTOR 2.813

CITESCORE 3.2

Article

The Evolution of a Higher-Dimensional FRW Universe with Variable G and Λ and Particle Creation

Alnadhief H. A. Alfedeel

MDPI

https://doi.org/10.3390/universe9060255

universe

MDPI

Article

The Evolution of a Higher-Dimensional FRW Universe with Variable G and Λ and Particle Creation

Alnadhief H. A. Alfedeel [1,2,3]

[1] Department of Mathematics and Statistics, Imam Mohammad Ibn Saud Islamic University (IMSIU), Riyadh 13318, Saudi Arabia; aaalnadhief@imamu.edu.sa
[2] Department of Physics, Faculty of Science, University of Khartoum, P.O. Box 321, Khartoum 11115, Sudan
[3] Centre for Space Research, North-West University, Potchefstroom 2520, South Africa

Abstract: Using an open thermodynamic systems theory, the effect of particle creation on the evolution and dynamics of the standard cosmological FLRW model in a higher-dimensional spacetime with functionally dependent cosmological and gravitational constants Λ and G is investigated. The gravitational field equations have been transformed into a dimensionless system of non-linear, first-order, coupled differential equations (DEs) as functions of the universe's density parameters Ω_i and rate of particle creation Ψ in redshift space, which can be numerically casted. Two cosmological models are obtained, depending on the choice of particle creation rate—$\Psi \sim H^2$ and $\Psi \sim n^2$ for dust-, radiation- and dark-energy-dominated universes, respectively. The dynamic behaviour of each model is discussed.

Keywords: higher dimensions; varying G and Λ; particle creation

check for updates

Citation: Alfedeel, A.H.A. The Evolution of a Higher-Dimensional FRW Universe with Variable G and Λ and Particle Creation. *Universe* **2023**, *9*, 255. https://doi.org/10.3390/universe9060255

Academic Editors: Lorenzo Iorio and Panayiotis Stavrinos

Received: 19 March 2023
Revised: 12 May 2023
Accepted: 23 May 2023
Published: 26 May 2023

1. Introduction

Modern cosmologists and particle physicists have paid great attention in recent times to the study of higher-dimensional cosmological models in Einstein's field equations within the framework of time-varying gravitational and cosmological running constants. The fundamental hypothesis that the universe may have once existed in a higher-dimensional era makes the study of higher-dimensional (HD) spacetime crucial. The idea of higher dimensions was firstly used by Kaluza and Klein [1,2], who made the assumption that spacetime is five-dimensional to unify the general theory of relativity (GR) with electromagnetic theory (EMT). The HD theory can be used to examine the cosmology of the early universe because it contributes to our understanding of how fundamental constructions are time-dependent. Furthermore, it is assumed that the universe's four-dimensional spacetime is immersed in a higher-dimensional HD epoch and becomes four-dimensional at later times, which suggests that the dynamical phenomena cause the extra dimension to become undetectably small; see [3].

According to the current cosmological observations of type Ia supernovae [4–7], the universe is expanding at an accelerating rate. It is commonly accepted that the dark energy candidate Λ in Einstein's field equations is responsible for the cosmic acceleration of the universe. Cosmological observations reveal a significant discrepancy between the observed value of the cosmological constant and the theoretically expected value; consequently, one approach to closing this gap is to consider it as a dynamical quantity rather than as a pure constant. Given that the universe is expanding and the Newtonian gravitational constant G predominated in the early times, it is reasonable to consider G as a function of time. Such an assumption was put forth by P. Dirac [8,9]. Since then, several attempts have been made to formulate a theory of gravity that incorporates G as a time-varying function.

The notion of particle formation in the universe was firstly introduced by Prigogine et al. [10,11]. It is hypothesized that particle creation induces an additional pressure term,

p_c, that is similar to a bulk viscous material in the universe's usual energy monument tensor. It is believed that the decay of the false vacuum energy density Λ was responsible for the formation of particles and the production of entropy during the early stages of the universe's evolution; see [12,13]. Since Prigogine et al.'s notion was introduced, the study of particle creation in cosmology has interested many physicists [10,11,14–22]. For instance, Prigogine et al. [10,11] investigated how the thermodynamics of open systems in the context G and Λ affect particle formation rate. The gravitational field equations are solved using the universe's power law scale factor. Dixit et al. [15] examined particle creation in FLRW-type cosmological models with varying cosmological and gravitational constants. The required field equations are solved by assuming $q = \alpha + \beta H$, which results in a scale factor $a = exp[(1/\beta)\sqrt{2\beta t + k}]$ with a positive constants k. The time-dependent higher-dimensional field equations incorporate a general formulation of particle and entropy production. The physical parameters, the deceleration parameter q, particle creation rate, entropy S, cosmological constant, Newton's gravitational constant G and energy density have been evaluated. Except for G and S, all parameters decrease in all dimensions over time. Both G and S increase with time. Particle creation influences both early and late stages of the universe. The relevance of five-dimensional Kaluza–Klein FRW model solutions with and without particle production in radiation and matter-dominated phases is examined. In addition to that, in high-dimensional Friedman–Robertson–Walker (FRW) spacetime, Ref. [16] studied particle production under the assumption that the gravitational and cosmological running constants are variables. Two scale factor types are taken into consideration while solving the field equations $a(t) = \sqrt{t^\alpha e^t}$ and $a(t) = m\sqrt{\sinh(kt)}$; this results in two separate time-dependent deceleration parameters. Each model's physical parameters are discussed. Moreover, in line with the context of higher derivative theory, Singh et al. [17] explored how the particles' creation influenced the early universe's evolution within the spatially flat Friedman–Lemaitre–Robertson–Walker (FLRW) cosmological model. They treated the universe as an open thermodynamic system in which the formation of particles results in a negative pressure (p_c) plus the normal thermodynamic pressure (p).

Recently, the impact of particle creation upon the evolution of n-dimensional (FLRW) cosmological models using the functionally dependent gravitational G and cosmological Λ running constants were studied by [23]. The creation of new particles results in additional negative creation pressure in an open thermodynamic system of the universe. In this derived model, it was discovered that this pressure is insignificant. Geometric investigations of these cosmological findings and related observational constraints are conducted. Calvao et al. [18] re-examined Prigogine's phenomenological approach to matter creation in the cosmological context of a covariant formulation. They found that if the specific entropy changes, some of their results become invalid. Expressions for entropy production rate and temperature evolution equations are deduced and discussed. Moreover, a new flat cosmological scenario where the universe's acceleration is powered exclusively by the production of the cold dark matter (CDM) particles has been examined by Alcaniz et al. [19] and Steigman et al. [22]. However, parallel research that incorporates a non-standard cosmological model is investigated as well. For instant, Harko et al. [12] have investigated the effects of matter creation on the anisotropic Bianchi type-I spacetime evolution and dynamics. The author assumed two forms of particle creation rate Ψ, namely, (i) $\Psi \sim H^2$, "the square of the mean Hubble", and (ii) $\Psi \sim \rho$, "the fluid energy density". They then expressed a general solution to the gravitational field equations in an exact parametric form. They found that in the first case (model), the anisotropic cosmological models became isotropically flat as time progressed, while in the second model, the anisotropic universe did not isotropize and instead ended in a Kasner-type geometry.

Motivated by the preceding discussion, the purpose of this study is to investigate the dynamic behaviour of the FLRW model in a higher-dimensional spacetime with variables G and Λ and the matter creation process. In our solution processes, the gravitational field equation will be transformed into a system of dimensionless first-order, non-linear coupling differential equations (EDs), where it can be numerically integrated.

The paper's structure is as follows. In Section 2, we present the FRW metric and the field equations in a higher-dimensional spacetime with variables G and Λ and in terms of matter and entropy creation. In Section 3, the field equations are transformed into redshift space for numerical integrations. In Section 4, some particular models of interest are obtained. Section 5 is the conclusion of the work.

2. The Metric and Fields Equations

The homogeneous, isotropic Friedman–Robertson–Walker (FRW) metric in $(m+2)$ dimensional spacetime is given by:

$$ds^2 = dt^2 - a^2(t)\left[dr^2 + r^2 dx_m^2\right], \tag{1}$$

where $a(t)$ is scale factor, and dx_m^2:

$$dx_m^2 = d\theta_1^2 + \sin^2\theta_1 d\theta_2^2 + \cdots + \sin^2\theta_{m-1} d\theta_m^2. \tag{2}$$

We assume that the universe is filled with perfect fluid, whose the energy–momentum tensor is given by

$$T_{ij} = (\rho + p_e)u_i u_j - p_e g_{ij}, \tag{3}$$

where $p_e = p + p_c$, p is fluid pressure, p_c is particle creation pressure, ρ is the energy density, p is cosmic fluid pressure and u_i is the four-velocity vector satisfying $u_i u^j = 1$. Throughout this paper, we will consider that

$$p = w\rho,$$

where $w = [-1, 1]$. In this study, we consider

$$w = \begin{cases} 0 & \text{for dust} \\ 1/3 & \text{for radiation} \\ -1 & \text{for dark energy} \end{cases}$$

as an equation of state (EoS) parameter that relates the fluid pressure to its energy density ρ.

2.1. Thermodynamics Formulations

In this subsection, the thermodynamics' basics and particle creation will be highlighted and reviewed. Consider a system of volume V that has N particles inside it with internal energy E. The thermodynamic governing equations for this system are defined as follows:

$$p = \frac{n}{\dot{n}}\dot{\rho} - \rho, \tag{4}$$

$$d(\rho V) = -(p + p_c)dV, \tag{5}$$

$$p_c = -\frac{p+\rho}{n}\left[n + \frac{V}{\dot{V}}\dot{n}\right] = -\frac{p+\rho}{(m+1)nH}\Psi(t), \tag{6}$$

$$\frac{\dot{S}}{S} = \frac{\dot{N}}{N} = \frac{\dot{n}}{n} + \frac{\dot{V}}{V}, \tag{7}$$

where m is number of dimensions, ρ is the energy density, p is the thermodynamic pressure, p_c is the creation pressure, n is the particle number density, $N = nV$ is the total number of particles, Ψ is the matter creation rate and S is the entropy. For more details and comprehensive discussions on the mechanisms of particle creation and thermodynamics, see [10–12,21].

2.2. The EFEs

The Einstein field equations (EFEs) with time-independent gravitational constant G and cosmological constant Λ are:

$$G_{ij} = R_{ij} - \frac{1}{2} g_{ij} R = -\kappa G T_{ij} - \Lambda g_{ij}. \tag{8}$$

These equations are similar to those obtained from varying the Lagrangian in extra dimensions [24–27]. Here, $\kappa = 8\pi$, G_{ij}, R_{ij}, g_{ij} and R are the Einstein tensor, the Ricci tensor, the metric tensor and the Ricci scalar, respectively. Usually, it is considered that $G_N \approx G^m R_m^{-m}$, but throughout this paper, we will assume that the cosmological constant $\Lambda^m = \Lambda = \Lambda(t)$ and gravitational constant $G^m = G(t)$. Using Equations (1) and (3), the modified Einstein field equations are calculated as follows:

$$\frac{m(m+1)}{2}\left(\frac{\dot{a}}{a}\right)^2 = \kappa G(t)\rho + \Lambda(t)\,, \tag{9}$$

and

$$m\frac{\ddot{a}}{a} + \frac{m(m-1)}{2}\left(\frac{\dot{a}}{a}\right)^2 = -\kappa G(t)(p + p_c) + \Lambda(t)\,, \tag{10}$$

where a letter with a dot in the centre means a derivative with respect to the cosmic time. Equations (10) and (11) are known as the generalized Friedman equations in $m+2$-dimensional space. Adding Equations (9) and (10) and using the fact that $\dot{a}/a = H$ yields

$$\dot{H} = -(m+1)H^2 - \frac{\kappa G}{m}[\rho - (p + p_c)] + \frac{2\Lambda(t)}{m}, \tag{11}$$

if $m = 2$, these equations will switch back to the general form of the Friedman equation in $4 - dim$ spacetime. Generally, the sum of Equations (9) and (10) is equivalent to the Bianchi identity "$\nabla_i T_{ij} = 0$", which is proportional to the time variation of the cosmological constant "Λ" and the gravitational constant "G"; thus,

$$\kappa G\left[\dot{\rho} + (m+1)(p + p_c + \rho)\frac{\dot{a}}{a}\right] + \kappa\rho\dot{G} + \dot{\Lambda} = 0\,. \tag{12}$$

Assuming that the total matter content of the universe is conserved, Equation (12) can be split into two independent equations: the energy density evolution

$$\dot{\rho} + (m+1)(p + p_c + \rho)\frac{\dot{a}}{a} = 0 \tag{13}$$

and

$$\kappa\rho\dot{G} + \dot{\Lambda} = 0 \tag{14}$$

as an evolution equation for Λ and G. We see that the dynamics of the model in $m+2$-dimensional spacetime is governed by H, ρ, Λ and G, but the system of Equations (11), (14) and (15) only provide three equations; hence, an auxiliary equation is needed to complete the solution process. In doing so, dividing Equation (9) by $2/m(m+1)H^2$ gives

$$1 = \Omega_m + \Omega_\Lambda\,, \tag{15}$$

where

$$\Omega_m = \frac{2\kappa G\rho}{m(m+1)H^2}\,, \qquad \Omega_\Lambda = \frac{2\Lambda}{m(m+1)H^2}\,, \tag{16}$$

and their current values at redshift $z = 0$ are given by

$$\Omega_{m_0} = \frac{\kappa G_0 \rho_0}{3H_0^2} \,, \qquad \Omega_{\Lambda_0} = \frac{\Lambda_0}{3H_0^2} \,. \tag{17}$$

Then, differentiating Equation (15) with respect to time gives

$$0 = \dot{\Omega}_m + \dot{\Omega}_\Lambda \,. \tag{18}$$

This equation will be used with the other three DEs to complete the system for the numerical integration process.

The deceleration parameter q is defined in terms of the H Hubble parameter as

$$q = -1 - \frac{\dot{H}}{H^2} \,, \tag{19}$$

3. System of DEs in Redshift Space

Equations (11), (13), (14), (16) and (18) provide the dynamical equations of the FLRW model with time-dependent G and Λ in higher-dimensional space as follows:

$$\dot{H} = -(m+1)H^2 - \frac{\kappa G}{m}(\rho - p) + \frac{2\Lambda(t)}{m} + \frac{\kappa G}{m} p_c \,, \tag{20}$$

$$\dot{\Omega}_m = \left[-2\frac{\dot{H}}{H} + \frac{\dot{G}}{G} - (m+1)(1+w)H\right]\Omega_m - \frac{2\kappa G}{mH} p_c \,, \tag{21}$$

$$\dot{\Omega}_\Lambda = -\left[-2\frac{\dot{H}}{H} + \frac{\dot{G}}{G} - (m+1)(1+w)H\right]\Omega_m + \frac{2\kappa G}{mH} p_c \,, \tag{22}$$

$$\dot{G} = -\frac{G}{\Omega_m}\left[\dot{\Omega}_\Lambda + 2\frac{\dot{H}}{H}\Omega_\Lambda\right] , \tag{23}$$

$$\dot{n} = -(m+1)nH + \Psi(t) \,, \tag{24}$$

$$\dot{S} = S\left\{\frac{\dot{n}}{n} + \frac{\dot{V}}{V}\right\} . \tag{25}$$

The equations are coupled systems of first-order differential equations, which describe the evolution of the Hubble parameter H, the energy mass density Ω_m, the dark energy density Ω_Λ, the Newtonian constant G, the number of particles n and the entropy of the system S. The deceleration parameter in equation Equation (19) is given by:

$$q = -1 + \left\{(m+1) + \frac{\kappa G}{mH^2}(\rho - p) - \frac{2\Lambda(t)}{mH^2} - \frac{\kappa G}{mH^2} p_c\right\} . \tag{26}$$

In order to perform numerical implementations and compare the model with the existing observational data, we first transform any time-dependent quantity to redshift space using the following equation:

$$a = \frac{1}{1+z} \,, \qquad \frac{d}{dt} = -(1+z)H\frac{d}{dz} \,. \tag{27}$$

Then, the normalized parameters are defined as

$$h = \frac{H}{H_0} \,, \qquad g = \frac{G}{G_0} \,, \qquad \mathcal{N} = \frac{n}{n_0} \,, \quad \mathcal{S} = \frac{S}{S_0} \,,$$

where H_0, G_0, n_0 and S_0 are the values of Hubble parameter, Newtonian running constant, number of particles and entropy of the system at redshift $z = z_0$, respectively. Therefore, the above system of DEs (20)–(26) can be transformed into its dimensionless form in the redshift space as follows:

$$h' = \frac{(m+1)h}{1+z}\left[1+\frac{(1-w)}{2}\Omega_m-\Omega_\Lambda\right]+\frac{(1+w)\Omega_m}{2(1+z)\mathcal{N}}\,\frac{\Psi}{n_0H_0}, \tag{28}$$

$$\Omega_m' = \left[-2\frac{h'}{h}+\frac{g'}{g}+\frac{(m+1)(1+w)}{2(1+z)}\right]\Omega_m-\frac{(1+w)\Omega_m}{(1+z)\mathcal{N}}\,\frac{\Psi}{n_0H_0^2h}, \tag{29}$$

$$\Omega_\Lambda' = -\left[-2\frac{h'}{h}+\frac{g'}{g}+\frac{(m+1)(1+w)}{2(1+z)}\right]\Omega_m+\frac{(1+w)\Omega_m}{(1+z)\mathcal{N}}\,\frac{\Psi}{n_0H_0^2h}, \tag{30}$$

$$g' = -\frac{g}{\Omega_m}\left[\Omega_\Lambda'+2\frac{h'}{h}\Omega_\Lambda\right], \tag{31}$$

$$\mathcal{N}' = \frac{(m+1)}{(1+z)}\mathcal{N}-\frac{\Psi}{n_0H_0(1+z)h}, \tag{32}$$

$$\mathcal{S}' = \mathcal{S}\left\{\frac{\mathcal{N}'}{\mathcal{N}}+\frac{(m+1)}{1+z}\right\}, \tag{33}$$

$$q = -1+(m+1)\left\{1+\frac{(1-w)}{2}\Omega_m-\Omega_\Lambda+\Omega_m\frac{\Psi}{2n(1+m)H}\right\}. \tag{34}$$

Equations (28)–(34) are first-order, non-linear, coupled differential equations that describe the evolution of the rescaled Hubble parameter h, the mass density parameter Ω_m, the dark energy density parameter Ω_Λ, the Newtonian gravitational constant g, the number of particles $\mathcal{N}$ and the generated entropy of the system S in terms of the particle creation rate Ψ as a function of redshift z in a higher-dimensional spacetime.

4. Cosmological Models

This section displays a set of two cosmological models that are generated from the choice of the particle creation rate Ψ and the equation of state parameter $w = [0, 1/3. - 1]$.

4.1. Model I

We employ the ansatz of [10,11,18], which takes the following form of particle creation:

$$\Psi = \alpha H^2$$

where $\alpha \geq 0$ is constant, and its dimensionless transformation requires that $\alpha = n_0/H_0$. As a result, by applying this specific formula, the governing system of DEs in Equations (28)–(33) can be reduced to the following:

$$h' = \frac{(m+1)h}{1+z}\left[1+\frac{(1-w)}{2}\Omega_m-\Omega_\Lambda\right]+\frac{(1+w)}{2(1+z)}\,\frac{\Omega_m h^2}{\mathcal{N}}, \tag{35}$$

$$\Omega_m' = \left[-2\frac{h'}{h}+\frac{g'}{g}+\frac{(m+1)(1+w)}{2(1+z)}\right]\Omega_m-\frac{(1+w)}{2(1+z)}\,\frac{\Omega_m h}{\mathcal{N}}, \tag{36}$$

$$\Omega_\Lambda' = -\left[-2\frac{h'}{h}+\frac{g'}{g}+\frac{(m+1)(1+w)}{2(1+z)}\right]\Omega_m+\frac{(1+w)}{2(1+z)}\,\frac{\Omega_m h}{\mathcal{N}}, \tag{37}$$

$$g' = -\frac{g}{\Omega_m}\left[\Omega_\Lambda'+2\frac{h'}{h}\Omega_\Lambda\right], \tag{38}$$

$$\mathcal{N}' = \frac{(m+1)}{(1+z)}\mathcal{N}-\frac{h}{(1+z)}, \tag{39}$$

$$\mathcal{S}' = \mathcal{S}\left\{\frac{\mathcal{N}'}{\mathcal{N}}+\frac{(m+1)}{1+z}\right\}, \tag{40}$$

$$q = -1+(m+1)\left\{1+\frac{(1-w)}{2}\Omega_m-\Omega_\Lambda+\frac{(1+w)}{2}\,\frac{\Omega_m h^2}{(1+m)\mathcal{N}}\right\}. \tag{41}$$

To show the impact of particle creation pressure p_c on the universe evolution of Model I, we have numerically integrated the above set of DEs in parallel using $h(z_0) = 1$,

$\Omega_m(z_0) = 0.3$, $\Omega_\Lambda(z_0) = 0.689$, $g(z_0) = 1$, $\mathcal{N}(z_0) = 1$ and $\mathcal{S}(z_0) = 1$ as initial conditions and employing the Runge–Kutta forth-order method for $m = 2$, as shown in Figure 1. We observe that all model physical parameters, with the exception of the deceleration parameter q, which demonstrates that when p_c is applied to the system, q always remains negative and starts at -1 and reaches -0.2 at the present time (at $z_0 = 0$), are consistent with the most recent cosmological data—an accelerating expansion of the universe. The Newtonian running constant, g, increases asymptotically until it reaches 1. As the universe expands, the induced particle pressure reduces the amplitude of the physical parameters.

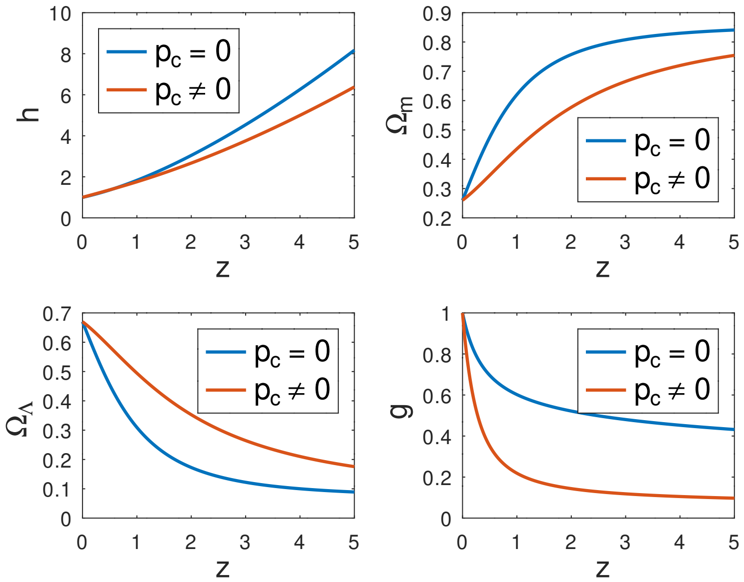

(**a**)

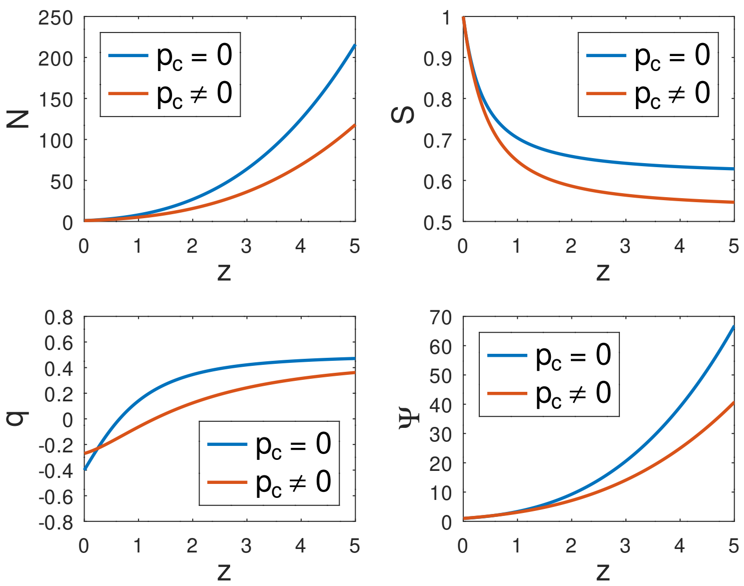

(**b**)

Figure 1. The **top** (**a**) and **bottom** (**b**) panels show the effects of pressure of particle creation p_c on the variation in the normalized Hubble parameter h, the energy density parameter Ω_m, the dark energy density parameter Ω_Λ, the normalized Newtonian constant g, the normalized total particle number $\mathcal{N}$, the normalized entropy $\mathcal{S}$, the deceleration parameter q and the matter creation rate Ψ for a time-varying G and Λ FLRW cosmological model with redshift. The initial conditions $h(z_0) = 1$, $\Omega_m(z_0) = 0.3$, $\Omega_\Lambda(z_0) = 0.689$, $g(z_0) = 1$, $\mathcal{N}(z_0) = 1$ and $\mathcal{S}(z_0) = 1$ and $w = 0$ are used with the Runge–Kutta method to integrate the model.

Figures 2–4 illustrates the numerical integration results of Model I in higher-dimensional spacetime. We can see that the following physical parameters agree with their expected values from the cosmological data: h, Ω_m, Ω_Λ, $\mathcal{N}$, $\mathcal{S}$, Ψ, and g. q behaves differently depending on the number of spaces and EoS w. For example, for a matter-dominated universe, when $w = 0$, if m is equal to 2 and 3, q takes on a negative values less than -0.5, and the universe accelerates. On the other hand, if m is equal to 4 and 5, q takes positive values between 0.1 and 0.5, and the universe decelerates for a radiation-dominated universe when $w = 1/3$; if $m = 2$, q changes its sign from positive in the past to a negative value in the present time at $z = 0$, and if m = 3, 4, and 5, q remains positive and gradually decreases to its current approximated values $[0.145, 0.39, 0.69]$, respectively. Finally, for a dark energy type of fluid, when $w = -1$, if $m = [2, 3, 4, 5]$, q is constant and takes the values $[-0.78, -0.71, -0.65, -0.58,]$, respectively.

Dust

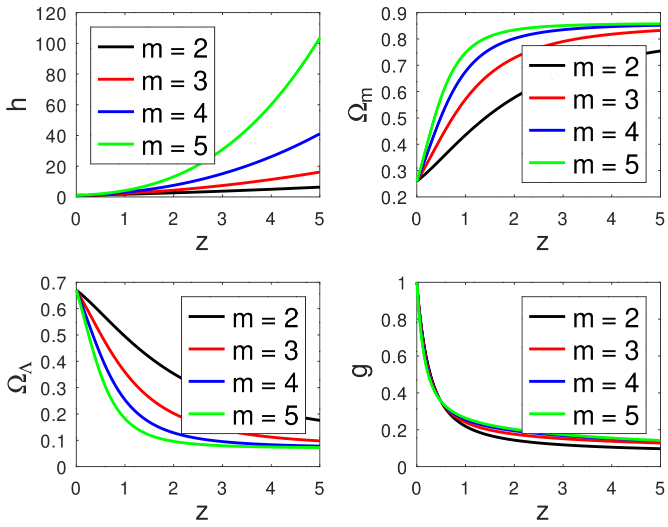

(**a**)

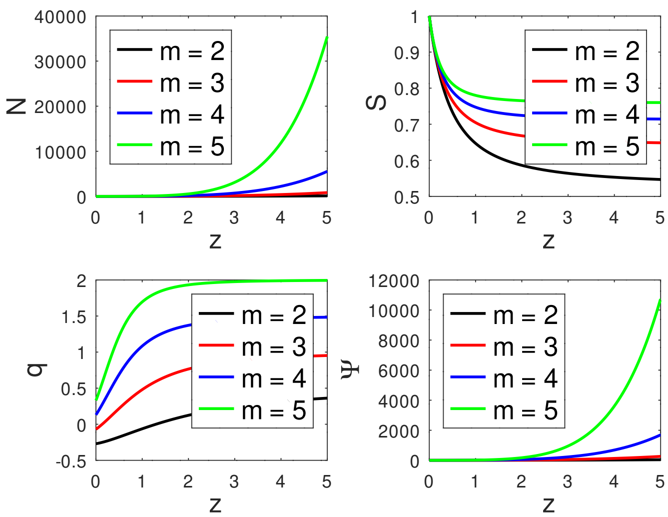

(**b**)

Figure 2. The **top** (**a**) and **bottom** (**b**) panels are the variations in $h, \Omega_m, \Omega_\Lambda, g, \mathcal{N}, \mathcal{S}, q,$ & Ψ for dust particles ($w = 0$) vs. redshift in terms of particle creation. The initial conditions $h(z_0) = 1$, $\Omega_m(z_0) = 0.3$, $\Omega_\Lambda(z_0) = 0.689$, $g(z_0) = 1$, $\mathcal{N}(z_0) = 1$ and $\mathcal{S}(z_0) = 1$ and different values of m are used with the Runge–Kutta method to integrate the governing DEs of Model I. (**a**) h, Ω_m, Ω_Λ and g vs. z (**b**) $\mathcal{N}$, $\mathcal{S}$, q and Ψ vs. z.

Radiation

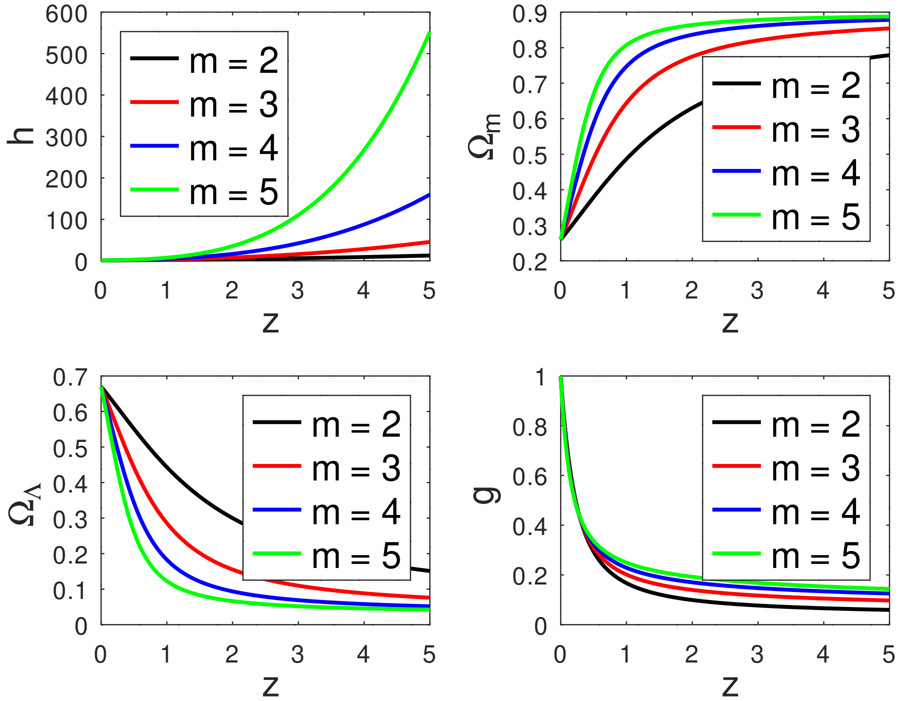

(**a**)

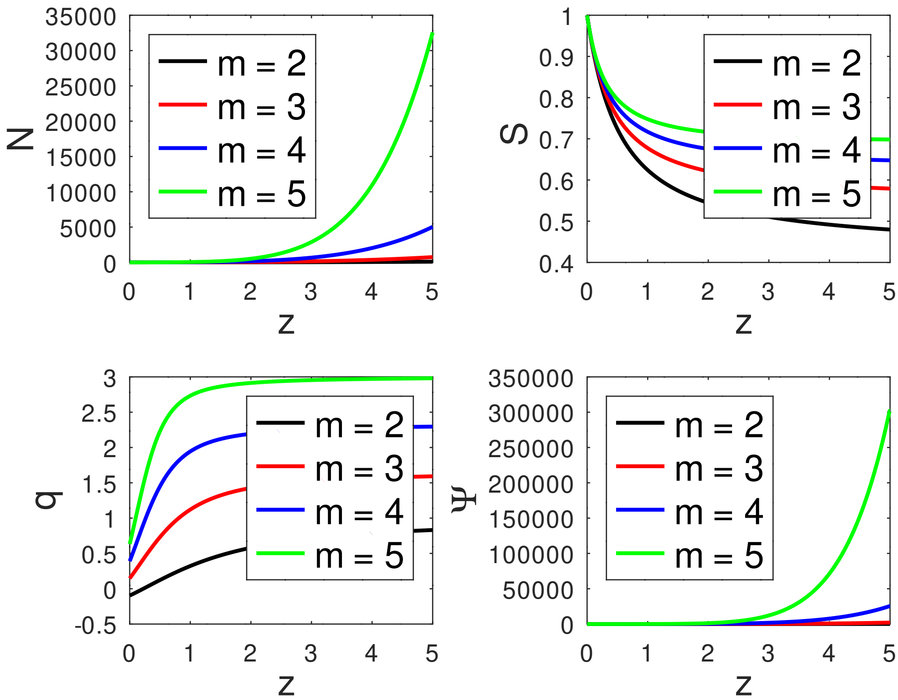

(**b**)

Figure 3. The **top** (**a**) and **bottom** (**b**) panels are the variations in $h, \Omega_m, \Omega_\Lambda, g, \mathcal{N}, \mathcal{S}, q,$ & Ψ for radiation-dominated fluid ($w = 1/3$) vs. redshift in terms of particle creation. The initial conditions $h(z_0) = 1$, $\Omega_m(z_0) = 0.3$, $\Omega_\Lambda(z_0) = 0.689$, $g(z_0) = 1$, $\mathcal{N}(z_0) = 1$ and $\mathcal{S}(z_0) = 1$, $w = 0$ and different values of m are used with the Runge–Kutta method to integrate the governing DEs of Model I. (**a**) h, Ω_m, Ω_Λ and g vs. z. (**b**) $\mathcal{N}$, $\mathcal{S}$, q and Ψ vs. z.

Dark Energy

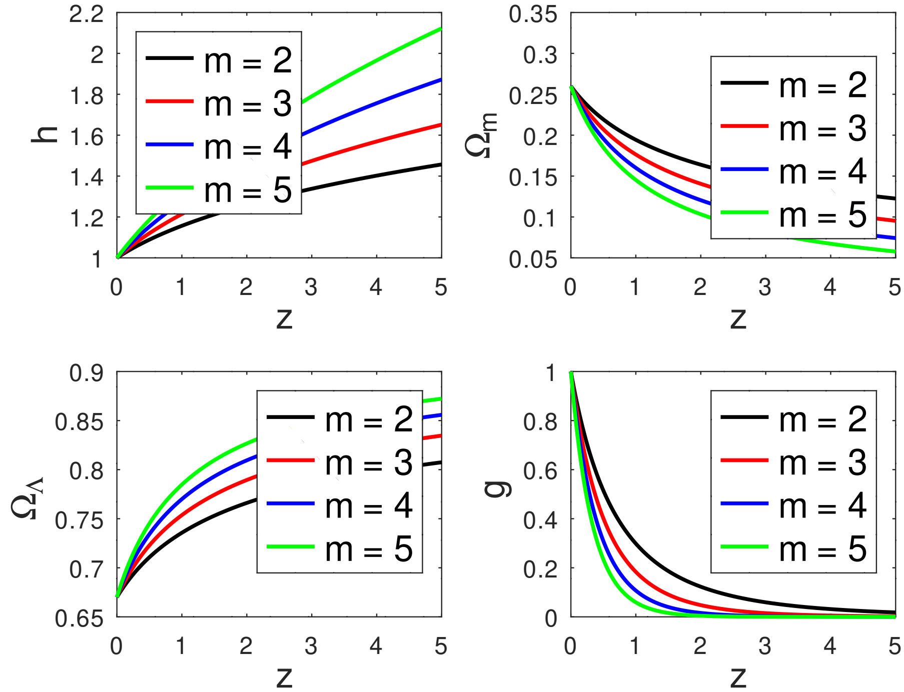

(**a**)

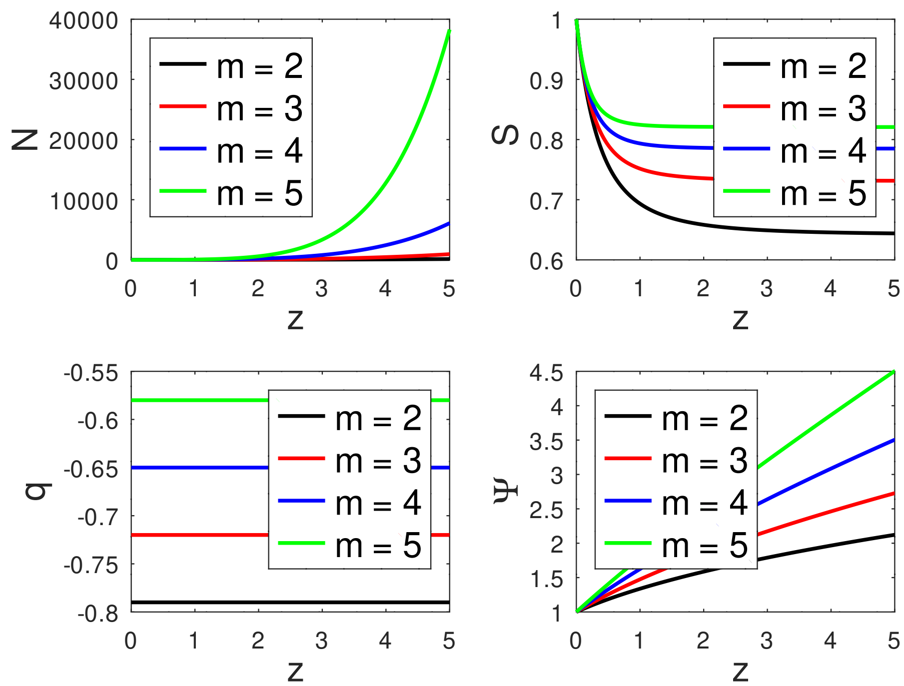

(**b**)

Figure 4. The **top** (**a**) and **bottom** (**b**) panels are the variations in $h, \Omega_m, \Omega_\Lambda, g, \mathcal{N}, \mathcal{S}, q,$ & Ψ for dark-energy-type fluids (w =-1) vs. redshift in terms of particle creation. The initial conditions $h(z_0) = 1$, $\Omega_m(z_0) = 0.3$, $\Omega_\Lambda(z_0) = 0.689$, $g(z_0) = 1$, $\mathcal{N}(z_0) = 1$ and $\mathcal{S}(z_0) = 1$, $w = 0$ and different values of m are used with the Runge–Kutta method to integrate the governing DEs of Model I. (**a**) h, Ω_m, Ω_Λ and g vs. z. (**b**) $\mathcal{N}$, $\mathcal{S}$, q and Ψ vs. z.

4.2. Model II

In this model, we assume that

$$\Psi = \Psi_0 n^2 = (H_0/n_0)n^2 \,.$$

With this assumption, the governing DEs in Equations (28)–(33) become

$$h' = \frac{(m+1)h}{1+z}\left[1+\frac{(1-w)}{2}\Omega_m - \Omega_\Lambda\right] + \frac{(1+w)}{2(1+z)}\,\Omega_m\mathcal{N}\,, \tag{42}$$

$$\Omega_m' = \left[-2\frac{h'}{h}+\frac{g'}{g}+\frac{(m+1)(1+w)}{2(1+z)}\right]\Omega_m - \frac{(1+w)}{2(1+z)}\,\frac{\Omega_m\mathcal{N}}{h}\,, \tag{43}$$

$$\Omega_\Lambda' = -\left[-2\frac{h'}{h}+\frac{g'}{g}+\frac{(m+1)(1+w)}{2(1+z)}\right]\Omega_m + \frac{(1+w)}{2(1+z)}\,\frac{\Omega_m\mathcal{N}}{h}\,, \tag{44}$$

$$g' = -\frac{g}{\Omega_m}\left[\Omega_\Lambda' + 2\frac{h'}{h}\Omega_\Lambda\right], \tag{45}$$

$$\mathcal{N}' = \frac{(m+1)\,\mathcal{N}}{(1+z)} - \frac{\mathcal{N}^2}{h(1+z)}\,, \tag{46}$$

$$\mathcal{S}' = \mathcal{S}\left\{\frac{\mathcal{N}'}{\mathcal{N}} + \frac{(m+1)}{1+z}\right\}, \tag{47}$$

$$q = -1+(1+m)\left\{1+\frac{(1-w)}{2}\Omega_m - \Omega_\Lambda + \frac{(1+w)}{2(1+m)}\,\Omega_m\mathcal{N}\right\}. \tag{48}$$

In order to depict the effect of the particle creation pressure p_c on the the universe's evolution discussed in Model II, we numerically integrated Equations (42)–(47) using $w = 0$ and the initial conditions $h(z_0) = 1$, $\Omega_m(z_0) = 0.3$, $\Omega_\Lambda(z_0) = 0.689$, $g(z_0) = 1$, $\mathcal{N}(z_0) = 1$ and $\mathcal{S}(z_0) = 1$ from the Planck [28] and the Runge–Kutta method. In Figure 5a,b, the blue and red solid lines show the variation in the normalized Hubble parameter h, the energy density parameter Ω_m, the dark energy density parameter Ω_Λ, the normalized Newtonian constant g, the normalized total particle number $\mathcal{N}$, the normalized entropy $\mathcal{S}$, the deceleration parameter q and the matter creation rate Ψ for an FLRW cosmological model with time-varying G and Λ with redshift z. We note that all models' physical parameters $h, \Omega_m, \Omega_\Lambda, N, S$, and Ψ are consistent with their expected observational values, except the deceleration parameter q, which shows that when p_c is imposed on the system, q always remains negative, starting from -1 and reaching -0.2 now (at $z_0 = 0$)—a universe expanding and accelerating. The Newtonian running constant g increases asymptotically, reaching the value of 1.

Figures 6–8 show the numerical integration results of Model II in higher-dimensional spacetime for different values of $m = [2,3,4,5]$ and EoS $w = [0, 1/3, -1]$. We see that $h, \Omega_m, \Omega_\Lambda, N, S, \Psi$, and g are in agreement with the observational data. q behaves differently depending on the value of space m and w. For instance, for a matter-dominated universe, if m equals 2, 3 or 4, q takes negative values between -0.033 and -0.4, and the universe expands with negative acceleration; if $m = 5$, q changes sign from negative in the past to a positive value at $z_0 = 0$ for a radiation-dominated universe when $w = 1/3$; if $m = 2$, q is negative and asymptotically evolves to rich -1 for large values of z; if $m = 3, 4, 5$, q flips signs from being negative in the past to positive values of $0.055, 0.26$ and 0.49 at the current value of z; finally, for a dark-energy-dominated universe, when $w = -1$, $q = [-0.97, -0.975, -0.980, -0.985]$ for $m = [2,3,4,5]$, respectively, and the universe expands with a constant rate of acceleration.

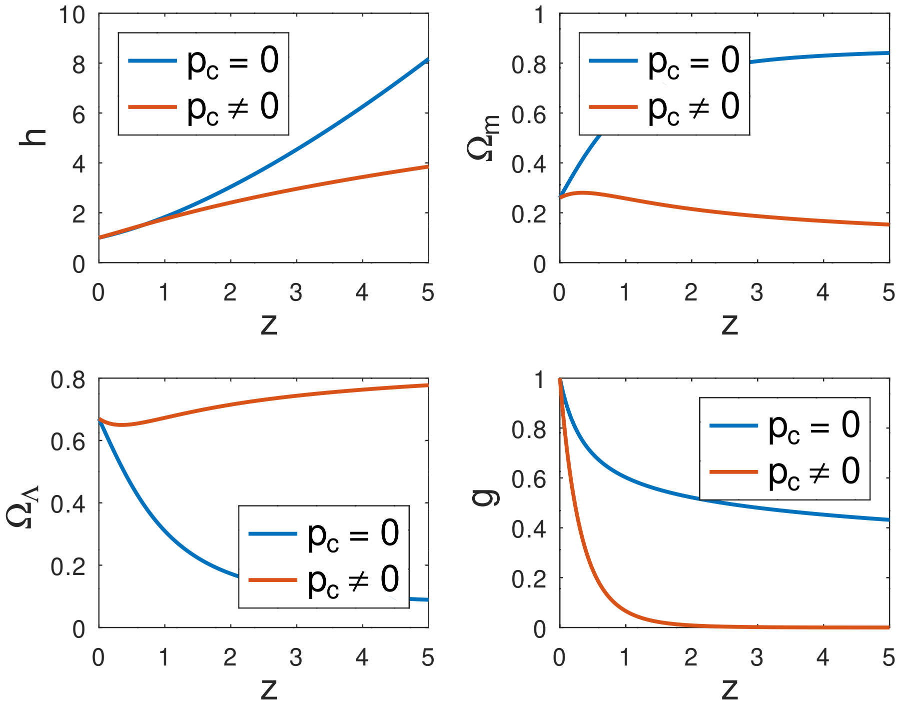

(**a**)

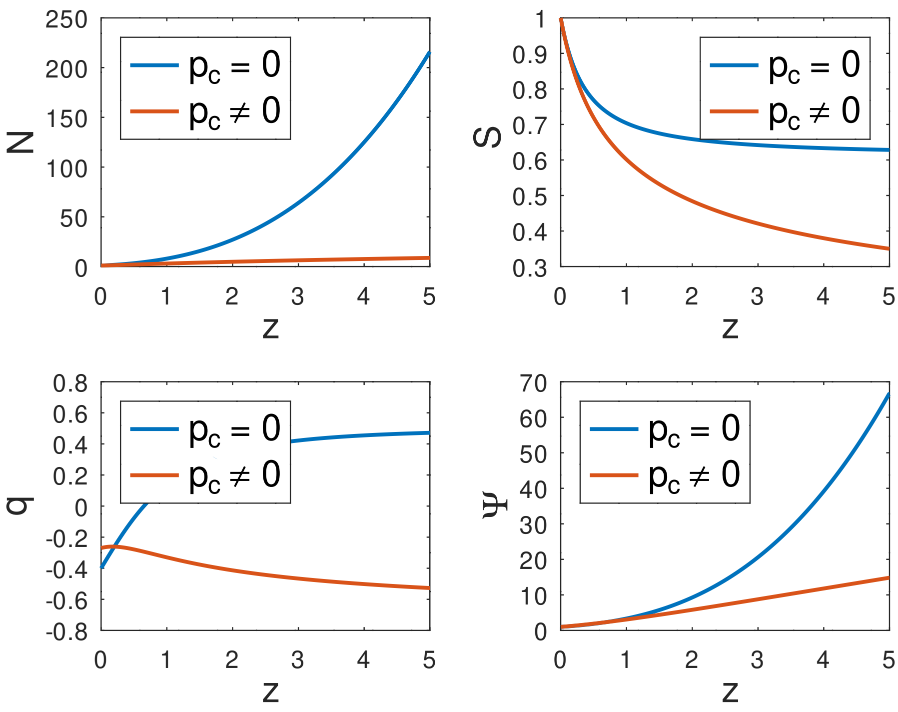

(**b**)

Figure 5. The **top** (**a**) and **bottom** (**b**) panels shows effect of the pressure particle creation p_c for Model II ($\Psi = \Psi_0 n^2$) on the variation in the normalized Hubble parameter h, the energy density parameter Ω_m, the dark energy density parameter Ω_Λ, the normalized Newtonian constant g, the normalized total particle number $\mathcal{N}$, the normalized entropy $\mathcal{S}$, the deceleration parameter q and the matter creation rate Ψ for a time-varying G and Λ FLRW cosmological model with redshift. The initial conditions $h(z_0) = 1$, $\Omega_m(z_0) = 0.3$, $\Omega_\Lambda(z_0) = 0.689$, $g(z_0) = 1$, $\mathcal{N}(z_0) = 1$ and $\mathcal{S}(z_0) = 1$ are used with the Runge–Kutta method to integrate the model equations.

Dust

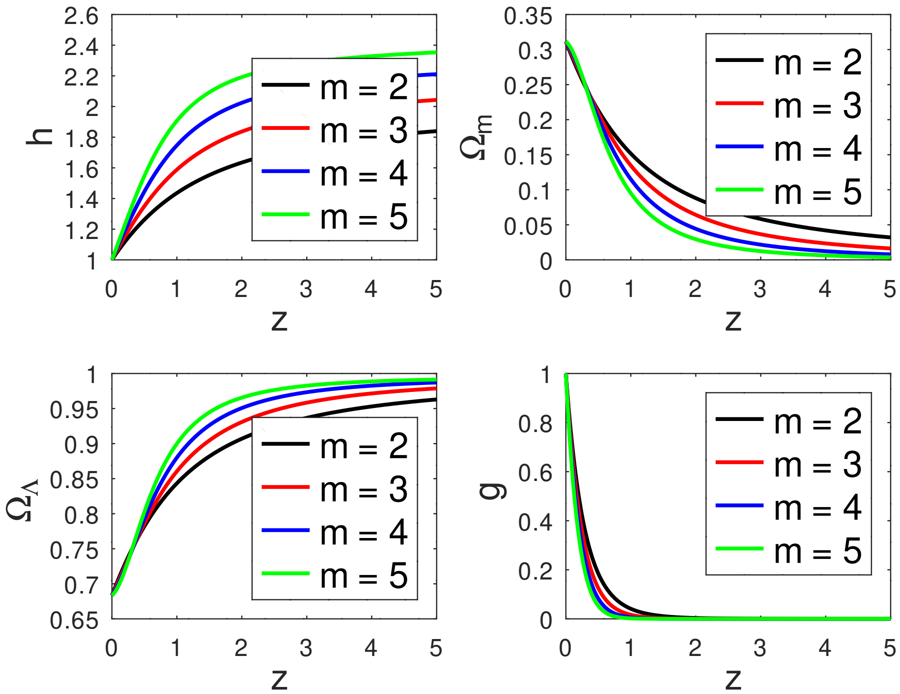

(**a**)

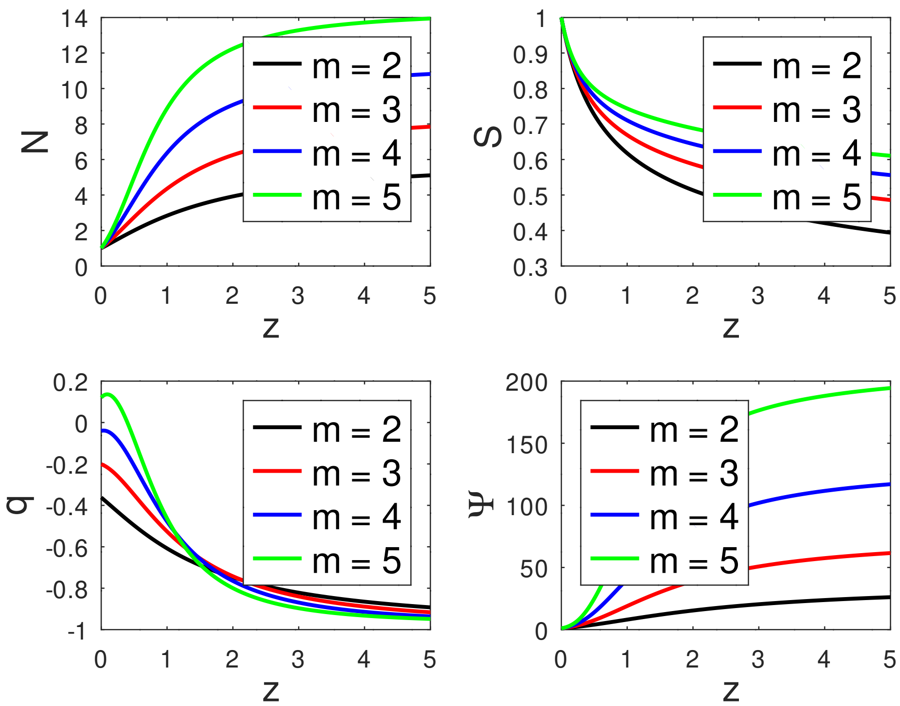

(**b**)

Figure 6. The **top** (**a**) and **bottom** (**b**) panels are the variations in $h, \Omega_m, \Omega_\Lambda, g, \mathcal{N}, \mathcal{S}, q,$ & Ψ for a matter-dominated universe ($w = 0$) vs. redshift in terms of particle creation. The initial conditions $h(z_0) = 1$, $\Omega_m(z_0) = 0.3$, $\Omega_\Lambda(z_0) = 0.689$, $g(z_0) = 1$, $\mathcal{N}(z_0) = 1$ and $\mathcal{S}(z_0) = 1$ and different values of m are used with the Runge–Kutta method to integrate the governing system of equations of Model II. (**a**) h, Ω_m, Ω_Λ and g vs. z. (**b**) $\mathcal{N}$, $\mathcal{S}$, q and Ψ vs. z.

Radiation

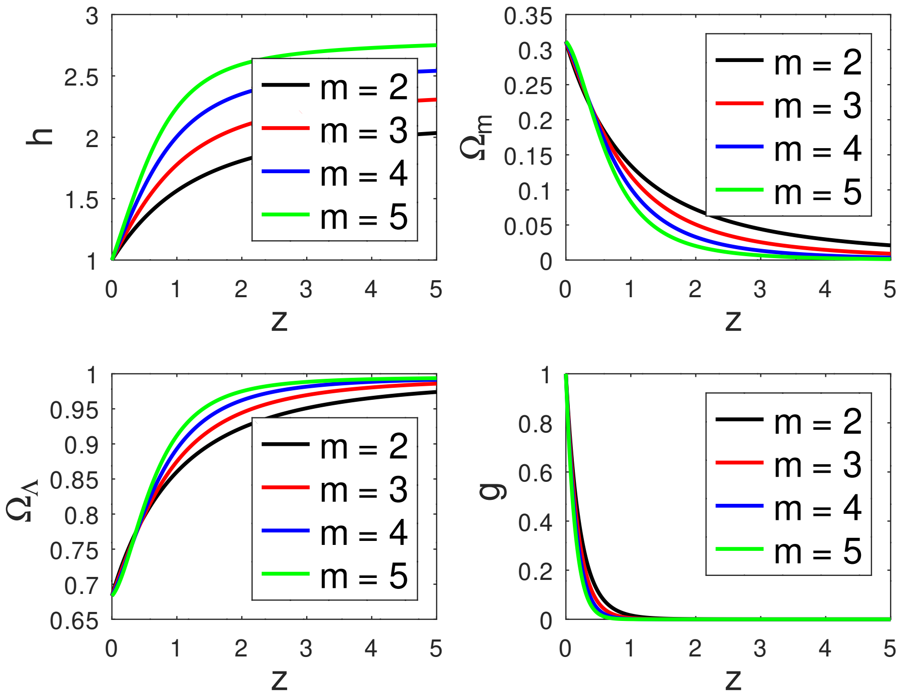

(**a**)

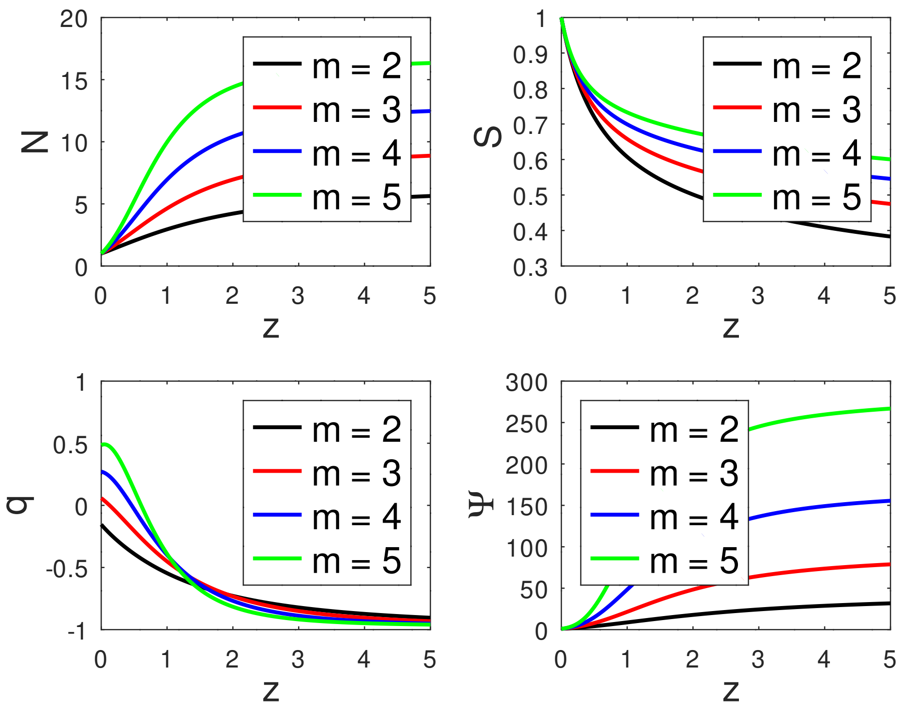

(**b**)

Figure 7. The **top** (**a**) and **bottom** (**b**) panels are the variations in $h, \Omega_m, \Omega_\Lambda, g, \mathcal{N}, \mathcal{S}, q,$ & Ψ for a radiation-dominated universe ($w = 1/3$) vs. redshift in terms of particle creation. The initial conditions $h(z_0) = 1$, $\Omega_m(z_0) = 0.3$, $\Omega_\Lambda(z_0) = 0.689$, $g(z_0) = 1$, $\mathcal{N}(z_0) = 1$ and $\mathcal{S}(z_0) = 1$ and different values of m are used with the Runge–Kutta method to integrate the governing system of equations of Model II. (**a**) h, Ω_m, Ω_Λ and g vs. z. (**b**) $\mathcal{N}$, $\mathcal{S}$, q and Ψ vs. z.

Dark Energy

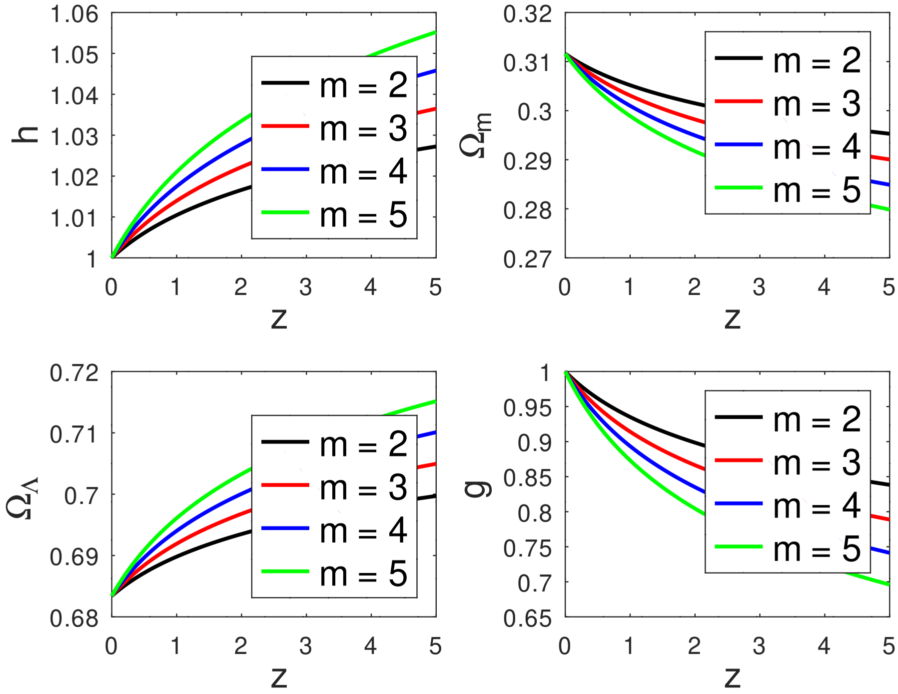

(**a**)

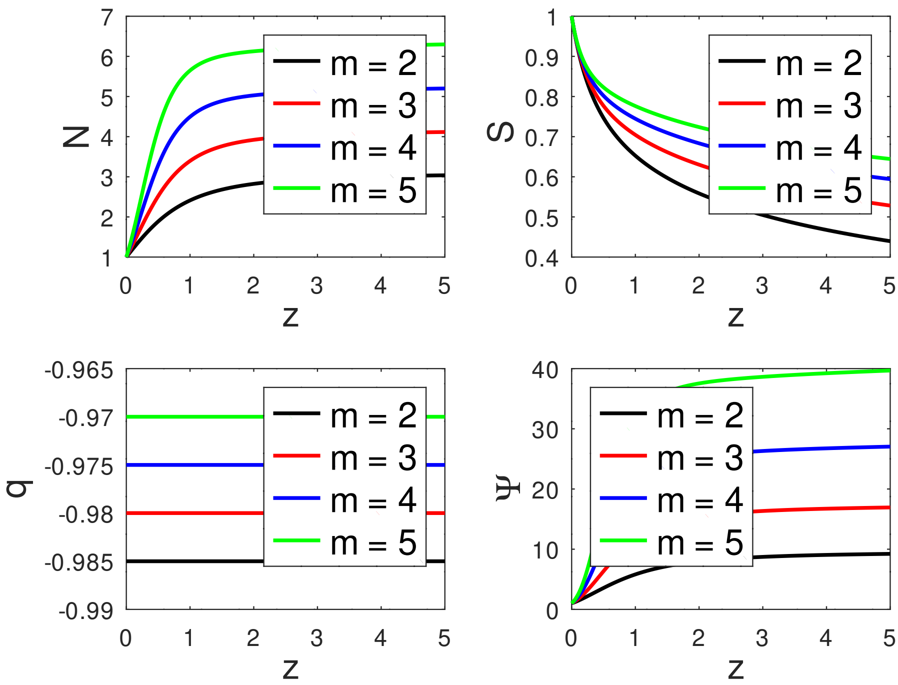

(**b**)

Figure 8. The **top** (**a**) and **bottom** (**b**) panels are the variations in $h, \Omega_m, \Omega_\Lambda, g, \mathcal{N}, \mathcal{S}, q,$ & Ψ for a dark-energy-dominated universe ($w = -1$) vs. redshift in terms of particle creation. The initial conditions $h(z_0) = 1$, $\Omega_m(z_0) = 0.3$, $\Omega_\Lambda(z_0) = 0.689$, $g(z_0) = 1$, $\mathcal{N}(z_0) = 1$ and $\mathcal{S}(z_0) = 1$ and different values of m are used with the Runge–Kutta method to integrate the governing system of equations of Model II. (**a**) h, Ω_m, Ω_Λ and g vs. z. (**b**) $\mathcal{N}$, $\mathcal{S}$, q and Ψ vs. z.

5. Conclusions

The purpose of this manuscript is to provide an explanation for the observed late-time acceleration in the universe's expansion rate by analysing the mechanism of particle creation in an open thermodynamic systems theory with functionally dependent gravitational constant G and cosmological constant Λ. The gravitational field equations have been transformed into a dimensionless system of a non-linear, first-order, coupled differential equation (DE) as function of universe's density parameters Ω_i and the rate of particle creation Ψ in redshift space and then numerically integrated using the Runge–Kutta method. A set of two cosmological models are obtained depending on the choice of the particle creation rate—$\Psi \sim H^2$ and $\Psi \sim n^2$ for dust-, radiation-, and dark-energy-dominated universes, respectively. We have generated three runs in which the universe in each model was dominated by matter $w = 0$, radiation $w = 1/3$ or dark energy $w = -1$, with different values of $m = 2, 3, 4, 5$ for "the number of dimensions". Accordingly, the following are observed:

- The values of h, Ω_m, Ω_Λ, $\mathcal{N}$, $\mathcal{S}$, Ψ and g are in agreement with their expected values today.
- In Model I, the behaviour of q changes depending w and m. For a matter-dominated universe, when $w = 0$, if m is equal to 2 and 3, q takes a negative values less than -0.5, and the universe accelerates; if m is equal to 4 and 5, q takes positive values between 0.1 and 0.5, and the universe decelerates; for a radiation-dominated universe, when $w = 1/3$, if $m = 2$, q changes sign from positive in the past to a negative value in the present time at $z = 0$, and if m = 3,4, and 5, q remains positive and gradually decreases to its current approximated values $[0.145, 0.39, 0.69]$, respectively; finally, for a dark energy type of fluid, when $w = -1$, if $m = [2, 3, 4, 5]$, q is constant and takes the values $[-0.78, -0.71, -0.65, -0.58]$, respectively.
- In Model II, it is observed that q behaves differently depending on the number of space m and w. For instance, for a matter-dominated universe, when $w = 0$, if m = 2, 3 and 4, q takes negative values between -0.033 and -0.4, the universe expands with negative acceleration, and if $m = 5$, q changes sign from $-ve$ in the past to a $+ve$ value at $z_0 = 0$. For a radiation-dominated universe, when $w = 1/3$, if $m = 2$, q is negative and asymptotically evolves to rich -1 for large values of z, if $m = 3, 4, 5$, q flips signs from negative in the past to the positive values 0.055, 0.26 and 0.49 at current value of z. Finally, for an energy-dominated universe, when $w = -1$, $q = [-0.97, -0.975, -0.980, -0.985]$ for $m = [2, 3, 4, 5]$, respectively, and the universe expands with a constant rate of acceleration.
- It is noted that, as the universe expands, the particle reduces the amplitude of the physical parameters.

These results are in good agreement with observations and similar to those obtained by [15]. We can expand this work in our upcoming study to determine the model-free parameters utilizing the available cosmological data.

Funding: The authors extend their appreciation to the Deanship of Scientific Research at Imam Mohammad Ibn Saud Islamic University (Riyadh, Saudi Arabia) for funding this work through Research Group no. RG-21-09-18.

Data Availability Statement: The data used in the study are available from the corresponding references.

Conflicts of Interest: The authors declare no conflicts of interest.

References

1. Kaluza, T. *Zum Unitätsproblem der Physik*. Sitzungsberichte der Königlich Preußischen Akademie der Wissenschaften: Berlin, Germany, 1921; pp. 966–972.
2. Klein, O. Quantentheorie und fünfdimensionale Relativitätstheorie. *Z. Phys.* **1926**, *37*, 895–906. [CrossRef]
3. Chodos, A.; Detweiler, S. Where has the fifth dimension gone? *Phys. Rev. D* **1980**, *21*, 2167. [CrossRef]

4. Perlmutter, S.; Gabi1, S.; Goldhaber, G.; Goobar, A.; Groom, D.E.; Hook, I.M.; Kim, A.G.; Kim, M.Y.; Lee1, J.C.; Pain, R.; et al. Measurements of the Cosmological Parameters Ω and Λ from the First Seven Supernovae at $z \geq 0.35$. *Astrophys. J.* **1997**, *483*, 565. [CrossRef]
5. Perlmutter, S.; Aldering, G.; Valle, M.D.; Deustua, S.; Ellis, R.S.; Fabbro, S.; Fruchter, A.; Goldhaber, G.; Groom, D.E.; Hook, I.M.; et al. Discovery of a supernova explosion at half the age of the Universe. *Nature* **1998**, *391*, 51–54. [CrossRef]
6. Perlmutter, S.; Aldering, G.; Goldhaber, G.; Knop, R.A.; Nugent, P.; Castro, P.G.; Deustua, S.; Fabbro, S.; Goobar, A.; Groom, D.E.; et al. Measurements of Ω and Λ from 42 high-redshift supernovae. *Astrophys. J.* **1999**, *517*, 565. [CrossRef]
7. Riess, A.G.; Filippenko, A.V.; Challis, P.; Clocchiatti, A.; Diercks, A.; Garnavich, P.M.; Gilliland, R.L.; Hogan, C.J.; Jha, S.; Kirshner, R.P.; et al. Observational evidence from supernovae for an accelerating universe and a cosmological constant. *Astron. J.* **1998**, *116*, 1009. [CrossRef]
8. Dirac, P.A. The cosmological constants. *Nature* **1937**, *139*, 323–323. [CrossRef]
9. Dirac, P.A.M. A new basis for cosmology. *Proc. R. Soc. Lond. Ser. A Math. Phys. Sci.* **1938**, *165*, 199–208. [CrossRef]
10. Prigogine, I.; Geheniau, J.; Gunzing, E.; Nardone, P. Thermodynamics of cosmological matter creation. *Proc. Natl. Acad. Sci. USA* **1988**, *85*, 7428. [CrossRef]
11. Prigogine, I.; Geheniau, J.; Gunzing, E.; Nardone, P. Thermodynamics and cosmology. *Gen. Relativ. Gravity* **1989**, *21*, 767. [CrossRef]
12. Harko, T.; Mak, M.K. Particle creation in cosmological models with varying gravitational and cosmological "constants". *Gen. Relativ. Gravit.* **1999**, *31*, 849–862. [CrossRef]
13. Mak, M.K.; Harko, T. Cosmological particle production in five-dimensional Kaluza-Klein theory. *Class. Quantum Gravity* **1999**, *16*, 4085. [CrossRef]
14. Singh, C.P.; Beesham, A. Particle creation in higher dimensional spacetime with variable *G* and Lambda. *Int. J. Theor. Phys.* **2012**, 51, 3951. [CrossRef]
15. Dixit, A.; Garg, P.; Pradhan, A. Particle creation in FLRW higher dimensional universe with gravitational and cosmological constants. *Can. J. Phys.* **2021**, *99*, 670–680. [CrossRef]
16. Sevinc, Ö.; Aydiner, E. Particle Creation in Friedmann-Robertson-Walker Universe. *Gravit. Cosmol.* **2019**, *25*, 397–406. [CrossRef]
17. Singh, G.P.; Beesham, A.; Deshpande, R.V. Particle production in higher derivative theory. *Pramana* **2000**, *54*, 729–736. [CrossRef]
18. Calvao, M.O.; Lima, J.A.S.; Waga, I. On the thermodynamics of matter creation in cosmology. *Phys. Lett. A* **1992**, *162*, 223. [CrossRef]
19. Alcaniz, J.S.; Lima, J.A.S. Closed and open FRW cosmologies with matter creation: Kine-matic tests. *Astron. Astrophys.* **1999**, *349*, 729.
20. Lima, J.A.S.; Silva, F.E.; Santos, R.C. Accelerating Cold Dark Matter Cosmology ($\Omega\Lambda \equiv 0$). *Class. Quant. Grav.* **2008**, *25*, 1. [CrossRef]
21. Lima, J.A.S.; Calvao, M.O.; Waga, I. *Cosmology, Thermodynamics and Matter Creation, Frontier Physics, Essay in Honor of Jayme Tiomno*; World Scientific: Singapore, 1990.
22. Steigman, G.; Santos, R.C.; Lima, J.A.S. An accelerating cosmology without dark energy. *Astropart. Phys.* **2009**, *6*, 33. [CrossRef]
23. Singh, S.S.; Chanu, S.K. Particle Production in Higher-Dimensional Universe with Time-Dependent Λ and G. *Braz. J. Phys.* **2021**, *51*, 1364–1370. [CrossRef]
24. Bronnikov, K.A.; Rubin, S.G. *Black Holes, Cosmology and Extra Dimensions*; World Scientific: Singapore, 2013.
25. Marciano, W.J. Time variation of the fundamental "constants" and Kaluza-Klein theories. *Phys. Rev. Lett.* **1984**, *52*, 489. [CrossRef]
26. Demaret, J.; Hanquin, J.L. Anisotropic Kaluza-Klein cosmologies. *Phys. Rev. D* **1985**, *31*, 258. [CrossRef]
27. Wesson, P.S. *Five-Dimensional Physics: Classical and Quantum Consequences of Kaluza-Klein Cosmology*; World Scientific: Singapore, 2006.
28. Aghanim, N.; Akrami, Y.; Ashdown, M.; Aumont, J.; Baccigalupi, C. Ballardini, M., et al. Planck 2018 results-VI. Cosmological parameters. *Astron. Astrophys.* **2020**, *641*, A6.